Advances in Concrete Construction, *Vol. 10, No. 4 (2020) 319-332*
DOI: https://doi.org/10.12989/acc.2020.10.4.319

Evaluate the effect of steel, polypropylene and recycled plastic fibers on concrete properties

Sabry Fayed and Walid Mansour*

Department of Civil Engineering, Faculty of Engineering, Kafrelsheikh University, Kafrelsheikh, Egypt

(*Received May 6, 2020, Revised August 17, 2020, Accepted September 11, 2020*)

Abstract. The impacts of reinforcing concrete matrix with steel fibers, polypropylene fibers and recycled plastic fibers using different volume fractions of 0.15%, 0.5%, 1.5% and 2.5% on the compressive and tensile characteristics are experimentally investigated in the current research. Also, flexural behavior of plain concrete (PC) beams, shear performance of reinforced concrete (RC) beams and compressive characteristics of both PC and RC columns reinforced with recycled plastic fibers were studied. The experimental results showed that the steel fibers improved the splitting tensile strength of concrete higher than both the polypropylene fibers and recycled plastic fibers. The end-hooked steel fibers had a positive effect on the compressive strength of concrete while, the polypropylene fibers, the recycled plastic fibers and the rounded steel fibers had a negative impact. Compressive strength of end-hooked steel fiber specimen with volume fraction of 2.5% exhibited the highest value among all tested samples of 32.48 MPa, 21.83% higher than the control specimen. The ultimate load, stiffness, ductility and failure patterns of PC and RC beams in addition to PC and RC columns strengthened with recycled plastic fibers enhanced remarkably compared to non-strengthened elements. The maximum ultimate load and stiffness of RC column reinforced with recycled plastic fibers with 1.5% volume fraction improved by 21 and 15%, respectively compared to non-reinforced RC column.

Keywords: mechanical properties; steel fiber; polypropylene fiber; recycled plastic fiber; beams; columns; deflection; deformation; elasticity modulus; crack pattern; toughness

1. Introduction

Recently, different types of fibers such as steel, aluminum, polypropylene, glass, plastic or even hybrid fibers have been used to enhance the concrete performance. The ideal fibers' characteristics can bridge and control cracks appearing in the reinforced concrete (RC) structural elements due to overloading or environmental assault (Lee *et al*. 2018). It is not easy to improve the mechanical characteristics of concrete structures significantly by incorporating fibers into the concrete matrix because behavior of fiber reinforced concrete (FRC) affected by volume fraction, aspect ratio, distribution, orientation and geometry of fibers (Thomas and Ramaswamy 2007, Al-Masoodi *et al*. 2016, Murthy and Ganesh 2019, Charron *et al*. 2020). On the other hand, the maximum size of coarse aggregate has a significant effect on the distribution of fibers in concrete matrix (Elices and Rocco 2008). Han *et al*. (2019) showed that the splitting tensile strength, the flexural strength and the fracture energy of steel fiber reinforced concrete (SFRC) increased as the steel fiber length increased while the compressive strength was hardly influenced. Also, the splitting tensile strength of SFRC increased with coarse aggregate maximum size up to 30 mm and then decreased. The inclusion of steel fibers into concrete improved the ductility in the compressive failure rather than the compressive strength (Bayramov *et al*. 2004).

The increase in the steel fiber content from 0.5% to 1.5% increased the tensile strength of concrete from 11% to 47% and increased the flexural strength from 3% to 124% (Abbas *et al*. 2018). The compressive strength of concrete poorly improved with the increase in steel fiber proportions contrary to the splitting tensile strength that noticeably improved (Pal *et al*. 2020). Song and Hwang (2004) improved the brittleness and strain capacities of high-strength concrete (HSC) by the addition of steel fibers with different ratios. The straight SFRC appeared higher tensile strength than the hooked ones because of the higher number of fiber-cement matrix interfaces. On the contrary, the hooked SFRC revealed superior performance in terms of ductility and toughness (Shi *et al*. 2020). Generally, end deformed steel fibers featured to be more efficient than those with deformations over the entire length (Trottier and Banthia 1994). At 0.5% steel fiber volume ratio, the stored energy of geopolymer cement concrete enhanced with 115.8% (Gomes *et al*. 2020), while the steel fiber dominated the unstable fracture toughness of steel fiber-reinforced rubberized concrete (Fu *et al*. 2019). Waste steel fibers affected the performance of concrete similar to the commercial ones (Sengul 2016, Grzymski *et al*. 2019). The workability of SFRC differed from that of plain concrete (PC) (Grünewald and Walraven 2001).

As the polypropylene fibers length increased, the cracking stress to axial tensile strength ratio of high

*Corresponding author, Assistant Professor
E-mail: waled_mansour@eng.kfs.edu.eg

http://www.techno-press.org/?journal=acc&subpage=7
ISSN: 2287-5301 (Print), 2287-531X (Online)

performance concrete decreased (Shen *et al*. 2020). Zhang *et al*. (2012) stated that the polypropylene fibers could improve the concrete's brittleness, but had a negative effect on the modulus of elasticity. The compressive strength of preplaced aggregate FRC reduced by adding waste polypropylene carpet fibers (Mohammadhosseini *et al*. 2020). On the other hand, the insertion of end looped aluminum fiber significantly enhanced both the compressive strength and the splitting tensile strength of concrete (Sabapathy *et al*. 2019). Pešić *et al*. (2016) investigated the effects of strengthening concrete with recycled plastic fibers of 0.4%, 0.75% and 1.25% volume fraction. Both the compressive strength and the elastic modulus of concrete were untouched while the tensile strength was significantly improved between 3% and 14% in the presence of plastic fibers. Cracking behavior of concrete structures improved as a result of using plastic fibers, but there was no possibility to enhance the load capacity (Ashok *et al*. 2020, Mohammed and Rahim 2020).

Different types of hybrid fibers were also employed to improve the mechanical properties of concrete matrix i.e., steel-basalt (Khan *et al*. 2020), steel-nylon (Akcay and Ozsar 2019), steel-polypropylene (Guo *et al*. 2019, Alwesabi *et al*. 2020, Zhong and Zhang 2020), steel-polyvinyl alcohol (Liu *et al*. 2020), steel-glass (Sivakumar and Santhanam 2007) and glass-basalt (Mazloom *et al*. 2020). Results showed that steel fibers added to concrete matrix could be substituted by a small extent of nonmetallic fibers to express toughness response similar to SFRC.

2. Research importance

Despite the aforementioned efforts, the impacts of steel fibers, polypropylene fibers and recycled plastic fibers of different volume fractions and geometry on the concrete properties were rarely studied in literature and further experimental investigations are required. The main objective of this paper is to assess the compressive strength, tensile strength and flexural strength of concrete matrix reinforced with steel and recycled plastic fibers of 0.5%, 1.5% and 2.5% volume fractions and polypropylene fibers of 0.15%, 0.5%, 1.5% and 2.5% volume fractions, respectively. A comparative evaluation of steel fibers, polypropylene fibers and recycled plastic fibers reinforced concretes was conducted based on performance and characteristics of hardened concrete; compressive, split tensile and flexural strengths. Moreover, the current research included the shear behavior of RC beams and compressive behavior of RC columns reinforced with recycled plastic fibers.

3. Experimental work

3.1 Materials properties

3.1.1 Concrete

All specimens were normal concrete (NC) that consisted of fine sand, crushed dolomite with maximum size of 10 mm, ordinary Portland cement (type 1, 42.5 R) and fresh water. Table 1 showed the concrete mix proportions. The targeted compressive strength of the NC was 30 MPa. Dry

Table 1 Concrete mix proportions (kg/m^3)

Item	Cement	Sand	Crushed dolomite	Water
Quantity	400	678.5	1258.7	199.5

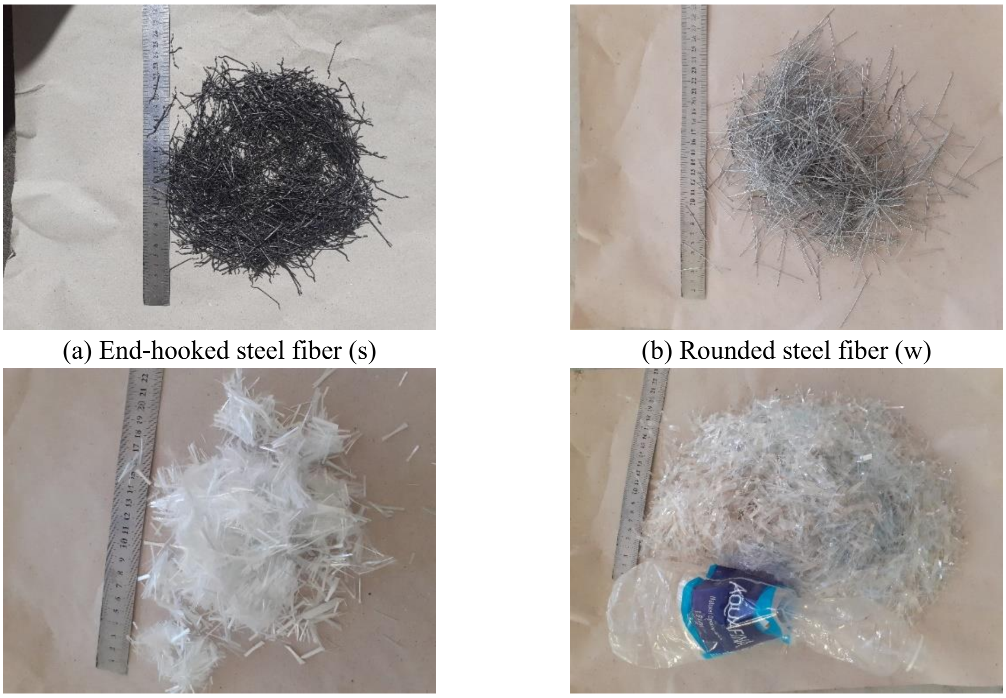

(a) End-hooked steel fiber (s)
(b) Rounded steel fiber (w)
(c) Polypropylene fiber (pp)
(d) Plastic fiber (p)

Fig. 1 The used fibers in the concrete

Table 2 Properties of the reinforcing bars

Bar	Type	Surface	Use	Poisson's ratio	Elastic modulus (GPa)	Yield stress (GPa)	Ultimate stress (GPa)	Elongation (%)
8 mm	NMS	Smooth	Columns	0.3	200	255.6	343.9	40
16 mm	HTS	Deformed	Beams	0.3	200	520.6	679.5	25

Table 3 The fibers properties

Fiber	Notation	Density (kg/m^3)	Diameter, *D* (mm)	Cross-section, *b***t* (mm*mm)	Length, *L* (mm)	Aspect ratio, *L*/(*D*, *b* or *t*)	Tensile strength (MPa)
End-hooked steel	S	7850	--	1.16*0.839	33.2	28.6, 39.6	1000
Rounded steel	w	7850	0.735	--	50 to 55	68, 74.8	1000
Polypropylene	PP	900	0.014	--	18	1285.7	350
Plastic	P	230	--	1 to 2 *0.42	20 to 25	20,10,47,25,12,60	105

ingredients were firstly mixed for three minutes followed by adding water, then the considered fibers were added and the mixture was well admixed for another two minutes.

3.1.2 Reinforcing rebar

Two different types of steel reinforcement bars were used in the experiments. The first type was normal mild steel (NMS) and used in the construction of the RC columns while the second one was high tensile steel (HTS) and used as a longitudinal tensile bars of the RC beams. To determine the mechanical properties of the used steel bars, the uniaxial tensile tests were carried out. Table 2 shows the mechanical properties of steel reinforcement bars. The test was carried out on two bars; 8 and 16 mm diameter. The 8 mm bar had smooth surface and made from NMS while the 16 mm bar had deformed surface and made from HTS.

3.1.3 Fibers

The fibers either metallic or nonmetallic type were used in the concrete to improve its mechanical properties. In this paper, both metallic and nonmetallic fibers were used. The end-hooked steel and the rounded steel fibers were added to the concrete as a metallic fiber. On the other hand, the polypropylene and the recycled plastic fibers were added to the concrete as a nonmetallic fiber. Recently, both the end-hooked steel and the polypropylene fibers were widespread while using the rounded steel and the plastic fibers to improve concrete properties were rarely studied. Both the end-hooked steel and the polypropylene fibers were commercial products while the rounded steel fiber was fabricated from the wire-wraps. The wire-wraps were used to correlate the steel bars together in the beams, columns, slabs, footing, etc. In addition, the wasted water bottles were cut to accroach the plastic fibers. The two ends of the water bottles were excluded because these ends were harder than the other parts. Fig. 1 shows the four fibers used in the current study. The end-hooked steel and the polypropylene fibers were ready products and were shown in Fig. 1(a) and Fig. 1(c), respectively. The rounded wire steel and the plastic fibers were fabricated and were shown in Fig. 1(b) and Fig. 1(d), respectively. The density, tensile strength and dimensions of the four fibers used were determined in the laboratory and were listed in Table 3.

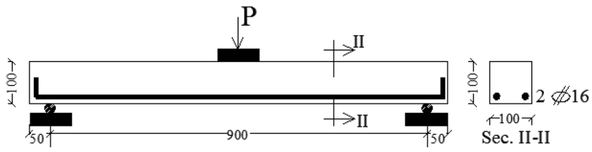

(a) Dimension and reinforcing of RC beams

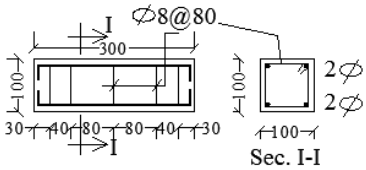

Longitudinal section

(b) Dimension and reinforcing of RC columns

RC beams PC beams

RC columns, cubes and cylinders

(c) Photo of the specimens after the casting process

Fig. 2 The specimens specification

Table 4 Details of the all tested specimens with the various fibers

Member	Group notation	Beam notation	Fiber type	Volume percentage of Fiber (%)	Fiber weight (gm)		Specimen specification	
					Per specimen	/m^3	Dimensions (mm)	Reinforcement
Cubic	--	C_0	No	No	No	No	100×100×100	No
	C_{pp}	$C_{pp0.15}$	pp	0.15	1.35	1350	100×100×100	No
		$C_{pp0.5}$		0.5	4.5	4500		
		$C_{pp1.5}$		1.5	13.5	13500		
		$C_{pp2.5}$		2.5	22.5	22500		
	C_p	$C_{p0.5}$	p	0.5	1.15	1150		
		$C_{p1.5}$		1.5	3.45	3450		
		$C_{p2.5}$		2.5	5.75	5750		
	C_s	$C_{s0.5}$	s	0.5	39.25	39250		
		$C_{s1.5}$		1.5	117.75	117750		
		$C_{s2.5}$		2.5	196.25	196250		
	C_w	$C_{w0.5}$	w	0.5	39.25	39250		
		$C_{w1.5}$		1.5	117.75	117750		
		$C_{w2.5}$		2.5	196.25	196250		
Cylinder	--	S_0	No	No	No	No	Diameter=150, Height=300	No
	S_{pp}	$S_{pp0.15}$	pp	0.15	7.15	1350	Diameter=150, Height=300	No
		$S_{pp0.5}$		0.5	23.85	4500		
		$S_{pp1.5}$		1.5	71.55	13500		
		$S_{pp2.5}$		2.5	119.25	22500		
	S_p	$S_{p0.5}$	p	0.5	6.09	1150		
		$S_{p1.5}$		1.5	18.28	3450		
		$S_{p2.5}$		2.5	30.47	5750		
	S_s	$S_{s0.5}$	s	0.5	208.02	39250		
		$S_{s1.5}$		1.5	624.07	117750		
		$S_{s2.5}$		2.5	1040.125	196250		
	S_w	$S_{w0.5}$	w	0.5	208.02	39250		
		$S_{w1.5}$		1.5	624.07	117750		
		$S_{w2.5}$		2.5	1040.125	196250		
PC beams	B_p	B_{p0}	No	No	No	No	100×100×650	No
		$B_{p0.5}$	p	0.5	7.5	1150	100×100×650	No
		$B_{p1.5}$		1.5	22.4	3450		
		$B_{p2.5}$		2.5	37.4	5750		
RC beams	B_R	B_{R0}	No	No	No	No	100×100×1000	Tensile bars=2Ø16
		$B_{R0.5}$	p	0.5	11.5	1150	100×100×1000	Tensile bars=2Ø16
		$B_{R1.5}$		1.5	34.5	3450		
		$B_{R2.5}$		2.5	57.5	5750		
PC columns	P_p	P_{p0}	No	No	No	No	100×100×300	No
		$P_{p1.5}$	p	1.5	10.35	3450	100×100×300	No
		$P_{p2.5}$		2.5	17.25	5750		
RC columns	P_R	P_{R0}	No	No	No	No	100×100×300	Longitudinal bars= 4Ø8, transverse stirrups=Ø8@80mm
		$P_{R1.5}$	p	1.5	10.35	3450		

3.2 Specimens specification

Experimental program consisted of 14 cubes, 14 cylinders, 3 PC columns, 2 RC columns, 4 PC beams, and 4 RC beams was prepared and tested. All specimens were casted using the same mix. Table 4 illustrates the specimen's details. The length of the cubic side was 100 mm while the diameter and the height of the cylinder were 150 and 300 mm, respectively. The total length of PC beams was 650 mm while the cross-section was 100×100 mm. Fig. 2 shows the casting sequence of specimens. RC beams had a cross-section of 100×100 mm with a total length of 1000 mm was designed to fail under shear. Two HTS bars of 16 mm diameter were used as a longitudinal tensile reinforcement. No transversal stirrups were developed to ensure shear failure as shown in Fig. 2(a). The cross-section of the RC and PC was similar and equal to 100×100 mm. The height of both PC and RC column was 300 mm. The longitudinal bars of RC column were 4Ø8 which made from NMS. The stirrups were 8 mm diameter spaced every 80 mm which made from NMS. The details and the photo of RC columns were illustrated in Fig. 2(b).

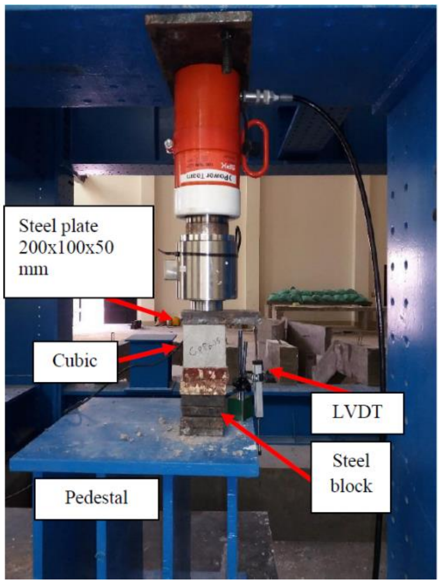

(a) Compression test on the cubes

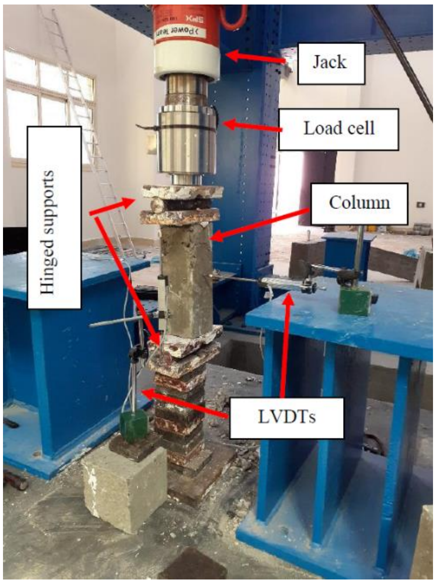

(b) Compression test on the columns

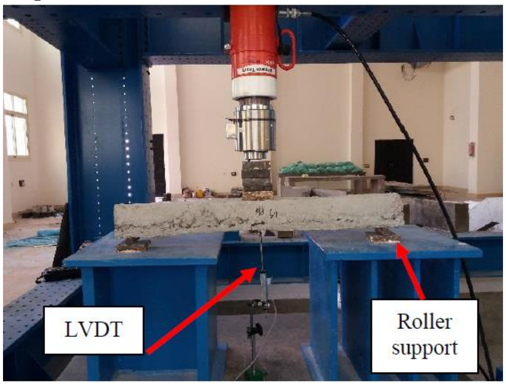

(c) Flexure test on the beams

(d) Splitting test on the cylinders

Fig. 3 The test setups and instrumentations of the specimens

Photo of all specimens after the casting process was shown in Fig. 2(c). As listed in Table 4, the cubes and cylinders were divided into four groups where the volume fraction of the four fibers was variable. A volume fraction of 0.5, 1.5 and 2.5% was carried out for all fiber type. In addition, a volume fraction of 0.15% was added for polypropylene fiber group. For the beams and the columns, the plastic fibers were added by a volume fraction of 0.5, 1.5 and 2.5%. The cubes, cylinders, beams and columns were covered by wet plastic sheets for 28 days then tested.

3.3 Set up and measurements

The test setups used for all specimens were shown in Fig. 3. A 1000 kN hydraulic jack was used to apply the force on the cubes, columns and the beams. A calibrated pressure transducer was positioned between the hydraulic jack and the specimen to measure the load with high accuracy. A linear variable displacement transducer (LVDT) was used to measure the displacements for the specimens. As shown in Fig. 3(a), the cubic was fixed between steel plates to avoid the local failure and for getting a uniform pressure. A LVDT was vertically put under the top steel plate to measure the vertical deformation (Δ). For testing the PC and RC columns, two hinged support were placed at the column ends to allow the rotation in the plane direction, as shown in Fig. 3(b). One LVDT was horizontally fixed at the mid height of the column to record the sway (Δ_h) while the second LVDT was vertically fixed at the column top to measure the shortening (Δ_v). The beams were tested under concentrated load at the mid span, as shown in Fig. 3(c). Two roller supports were used at the ends and LVDT was fixed at the mid span to record the deflection (Δ). The set up shown in Fig. 3(c) was used to test the plain beams. The effective span of PC and RC beams was 550 and 900 mm, respectively. The loading plate of 100×100×30 mm was used to prevent local crushing due to stress concentration. The splitting tensile test on the cylinders was carried out using a compression test machine with 2000 kN capacity, as shown in Fig. 3(d).

4. Results and discussion

4.1 Compression tests

4.1.1 Failure modes

Fig. 4 shows the failure modes of all cubes subjected to

(a) C_0

(b) Polypropylene cubes

(c) Plastic cubes

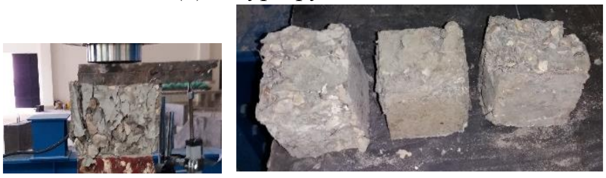

(d) End-hooked steel cubes

(e) Rounded wire steel cubes

Fig. 4 Failure modes of the cubes

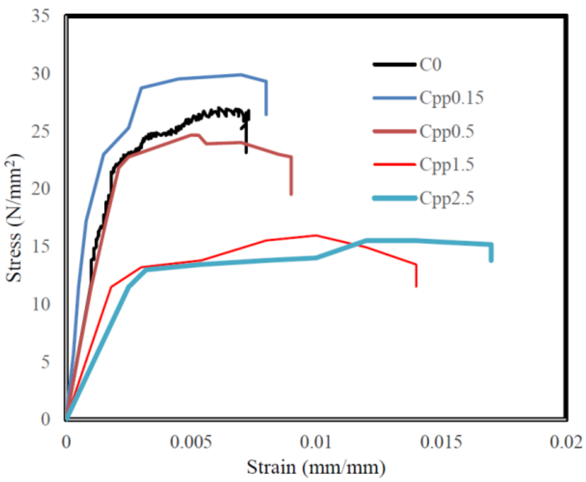

Fig. 5 Compressive stress-strain relationships of the fibrous cubes with the polypropylene

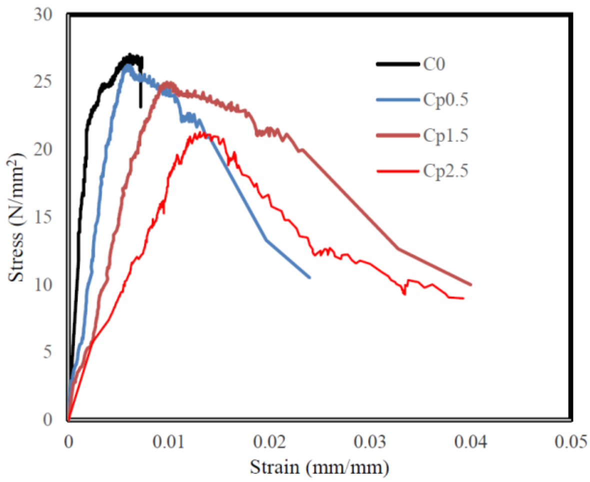

Fig. 6 Compressive stress-strain relationships of the fibrous cubes with the plastic

compression loads. All cubes did not crush at the maximum load except the control cube (C_0). For the C_0, two vertical cracks occurred at the maximum load, as shown in Fig. 4(a). As the load increased, the cube suddenly broke accompanied with high sound. For all fibrous cubes, many vertical cracks took placed before the crushing, in addition the failure occurred after the maximum load by several minutes. Also, the external concrete cover of the fibrous cubes was crushed due to high deformation. Cubes that containing recycled plastic fibers were the weakest compared to other fibrous cubes. As shown in Fig. 4(c), some of the plastic cubes were split. Cubes reinforced with polypropylene fibers were better than their counterparts reinforced with recycled plastic fibers, as shown in Fig. 4(b). The end-hooked and the rounded steel fiber cubes buckled to the external after the maximum load and achieved high deformation, as illustrated in Fig. 4(d) and Fig. 4(e). From the above, it is clear that the metallic and nonmetallic fiber improved the cubes collapse especially the metallic fiber either the end-hooked or the straight type due to preventing the sudden cubes collapse.

4.1.2 Stress-strain relationships

The applied load (P) versus the vertical shortening (Δ) were recorded for all cubes. The stress (f) was calculated using Eq. (1) while the strain (ε) was determined using Eq. (2).

$$f = \frac{P}{A} \quad (N/mm^2) \tag{1}$$

$$\varepsilon = \frac{\Delta}{L} \quad (mm/mm) \tag{2}$$

where A is the cross-section area of the cube (100×100 mm^2) and L is the cube height (100 mm). Stress-strain relationships were drawn for all cubes. The stress-strain curves of C_{pp}, C_p, C_s and C_w cubes were shown in Fig. 5, Fig. 6, Fig. 7 and Fig. 8, respectively. The resulted curves of all cubes were well investigated and were analyzed in Table 5. Table 5 lists the ultimate compressive strength

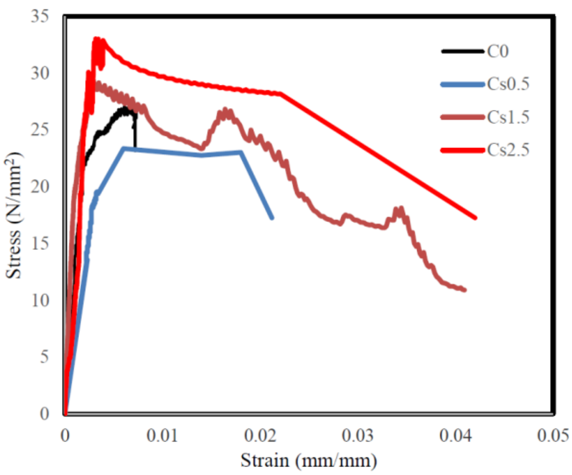

Fig. 7 Compressive stress-strain relationships of the fibrous cubes with the end-hooked steel

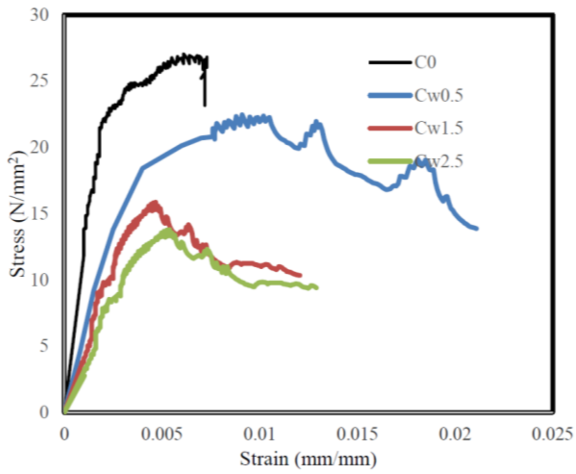

Fig. 8 Compressive stress-strain relationships of the fibrous cubes with the rounded wire steel

Table 5 Results analysis of the fibrous cubes under the compression

Group	Cubic designation	Volume fraction (%)	f_{cu} (N/mm^2)	Increase /decrease in f_{cu} (%)	ε_u	Increase in ε_u (%)	f_c* (N/mm^2)	ε*	Increase in ε* (%)	Toughness T (N/mm^2)	Increase in T (%)	E (N/mm^2)
--	C_0	No	26.66	--	0.0066	--	23.15	0.0072	--	0.17	--	11700
C_{pp}	$C_{pp0.15}$	0.15	29.9	12.15	0.003	-54.55	26.45	0.008	11.11	0.188	10.59	23000
	$C_{pp0.5}$	0.5	24.67	-7.46	0.0053	-19.70	19.55	0.009	25.00	0.189	11.18	11500
	$C_{pp1.5}$	1.5	15.97	-40.10	0.01	51.52	11.5	0.014	94.44	0.174	2.35	6388.889
	$C_{pp2.5}$	2.5	15.52	-41.79	0.012	81.82	13.8	0.017	136.11	0.207	21.76	4600
C_p	$C_{p0.5}$	0.5	25.86	-3.00	0.0062	-6.06	10.5	0.024	233.33	0.404	-137.65	5043.33
	$C_{p1.5}$	1.5	24.59	-7.76	0.01	51.52	10	0.04	455.56	0.642	277.65	3014.545
	$C_{p2.5}$	2.5	20.85	-21.79	0.0136	106.06	8.99	0.0393	445.83	0.525	208.82	1725.51
C_s	$C_{s0.5}$	0.5	23.34	-12.45	0.006	-9.09	17.25	0.021	191.67	0.41	141.18	6385.185
	$C_{s1.5}$	1.5	28.75	7.84	0.0031	-53.03	10.9	0.04	455.56	0.776	356.47	21444.81
	$C_{s2.5}$	2.5	32.48	21.83	0.0034	-48.48	17.25	0.042	483.33	1.015	497.06	11700
C_w	$C_{w0.5}$	0.5	22.17	-16.84	0.01	51.52	13.88	0.021	191.67	0.31	81.76	5520
	$C_{w1.5}$	1.5	15.58	-41.56	0.0048	-27.27	10.34	0.012	66.67	0.121	-28.82	3961.538
	$C_{w2.5}$	2.5	13.3	-50.11	0.0055	-16.67	9.4	0.0129	79.17	0.121	-28.82	3006.211

(f_{cu}), the ultimate strain (ε_u) at the ultimate compressive strength, the failure strength (f_c*), the failure strain (ε*), the toughness (T) and the elasticity modulus (E). The toughness was considered as the area under the stress-strain curve. It was noticed that the stress-strain curve was linear at the start so the E was easily determined by calculating the line slope at the beginning of the stress-strain curve. In the following sections, each group results will be separately discussed followed by a comparison between the fiber types.

4.1.2.1 The fibrous cubes with the polypropylene (C_{pp})

The cubes $C_{pp0.15}$ and $C_{pp0.5}$ induced an acceptable strength and elasticity modulus. The strength and the E of the $C_{pp0.15}$ were 12.15 and 96.58 % respectively higher than those of C_0. In addition, the strength and the E of the $C_{pp0.5}$ and C_0 were approximately identical. On the contrary, the strength of the cubes $C_{pp1.5}$ and $C_{pp2.5}$ was approximately 40% less than C_0. So that the volume fraction of the polypropylene exceeded 0.5% was not recommended. Although, using the polypropylene over 0.5 % decreased the strength, the failure strain and the toughness significantly increased. The failure strain of $C_{pp1.5}$ and $C_{pp2.5}$ was 94.44 and 136.11%, respectively higher than C_0. Moreover, the toughness of $C_{pp1.5}$ and $C_{pp2.5}$ was 2.35 and 21.76%, respectively higher than C_0. From the above, using the polypropylene with a volume fraction up to 0.5 % considered the optimum.

4.1.2.2 The fibrous cubes with the plastic (C_p)

It was noticed that the compressive strength of concrete cubes reinforced with recycled plastic fibers was less than the control specimen. The strength of $C_{p0.5}$, $C_{p1.5}$ and $C_{p2.5}$ was less than C_0 specimen by 3.00, 7.76 and 21.79%, respectively. The ultimate strain of $C_{p1.5}$ and $C_{p2.5}$ was 51.52 and 106.06%, respectively higher than C_0. Also, the failure strain of $C_{p0.5}$, $C_{p1.5}$ and $C_{p2.5}$ was higher than C_0 by 233.33, 455.56 and 445.83%, respectively. The $C_{p0.5}$, $C_{p1.5}$ and the $C_{p2.5}$ achieved toughness more than the C_0. So that using the plastic fibers considered a good admixture respect to the ductility. The elasticity modulus was significantly decreased with using the plastic fiber ratio. Consequently, use of recycled plastic fibers with volume fraction over

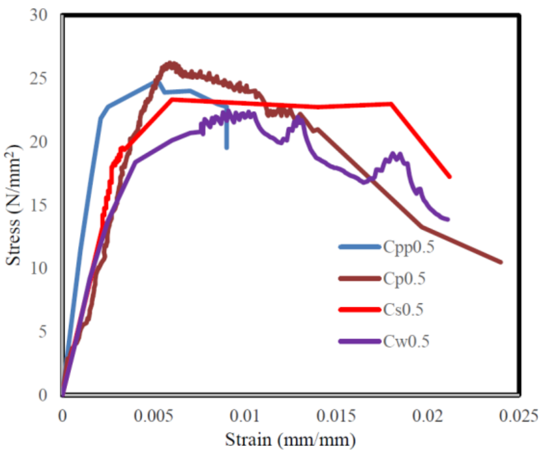

Fig. 9 Stress-strain curves of all fibrous cubes with a volume fraction of 0.5%

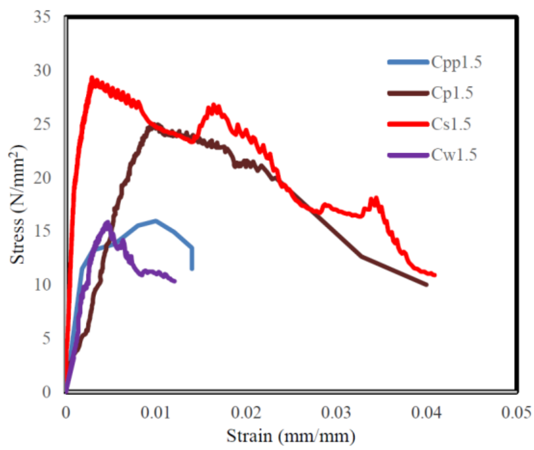

Fig. 10 Stress-strain curves of all fibrous cubes with a volume fraction of 1.5%

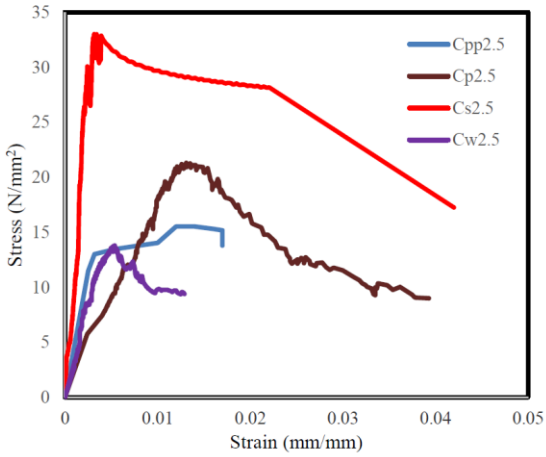

Fig. 11 Stress-strain curves of all fibrous cubes with a volume fraction of 2.5%

1.5% had a negative effect on the stiffness and the compressive strength.

4.1.2.3 The fibrous cubes with the end-hooked steel (C_s)

It was founded that the end-hooked steel fibers enhanced strength, failure strains and toughness of concrete in compression. The strength of $C_{s1.5}$ and $C_{s2.5}$ was higher than C_0 by 7.84 and 21.83%, respectively. The failure strain of $C_{s0.5}$, $C_{s1.5}$ and $C_{s2.5}$ was higher than C_0 by 191.67, 455.56 and 483.33%, respectively. The toughness of $C_{s0.5}$, $C_{s1.5}$ and $C_{s2.5}$ was higher than C_0 by 141.18, 356.47 and 497.06%, respectively. The end-hooked steel fiber with volume fraction over 0.5% had a significant influence on the compressive behavior of the concrete. In addition, the elasticity modulus (E) was similar for both the C_0 and $C_{s2.5}$ while the E of the $C_{s1.5}$ was 83.23% higher than the C_0. From the above results, the end-hooked steel fiber with a volume fraction over 0.5 % was considered as excellent admixture. Concrete compressive properties were significantly improved.

4.1.2.4 The fibrous cubes with the rounded wire steel (C_w)

The compressive strength of $C_{w0.5}$, $C_{w1.5}$ and $C_{w2.5}$ was less than that of C_0 by 16.84, 41.56 and 50.11%, respectively. All fibrous cubes reinforced with the rounded wire steel had a failure strain higher than C_0 while the E of such cubes decreased compared to C_0. The compressive response of $C_{w0.5}$ was significantly improved compared to $C_{w1.5}$ or $C_{w2.5}$. As the volume fraction of the rounded wire steel fiber decreased, the concrete compressive strength improved. It may referred to the fact that the bond between concrete matrix and smooth rounded wire steel fiber was weak due to absence of the end hooks or zagging. The steel wire fiber easily slipped out the concrete matrix compared to end-hooks fibers.

4.1.3 Comparison between fiber types

All stress-strain curves of all fibrous cubes with a volume fraction of 0.5, 1.5 and 2.5 % were drawn in Fig. 9, Fig. 10 and Fig. 11, respectively. It was shown that as the volume fraction increased, the difference between the four fibers significantly appeared. For 0.5% volume fraction, the strength of the plastic cubic was the highest, while the strength of the wired cube was the smallest. Also, the elasticity modulus of plastic, steel and wired cubic was approximately identical and less than the propylene cube. The toughness of the $C_{s0.5}$ was the highest while the toughness of the $C_{pp0.5}$ was the least. All cubes had good final strain except the propylene cube. Moreover, cubes reinforced with recycled plastic, end-hooked steel and rounded wire steel fibers exhibited similar ductility higher than cubes reinforced with propylene fibers. Results showed that among all fiber volume fractions, the compressive strength and toughness of concrete cubes reinforced with 0.5% volume fraction recorded the least standard deviation of the mean of 1.6 and 0.103, respectively.

For 1.5% volume fraction, the compressive strength and elasticity modulus of cubes reinforced with the end-hooked steel fiber recorded the highest values among all tested cubes. The toughness of the end-hooked steel fiber cube was the highest while the toughness of the the rounded steel fiber cube was the least. Also, the compressive strength of both the $C_{s1.5}$ and the $C_{p1.5}$ was higher than their counterparts reinforced with polypropylene and rounded steel fiber $C_{pp1.5}$

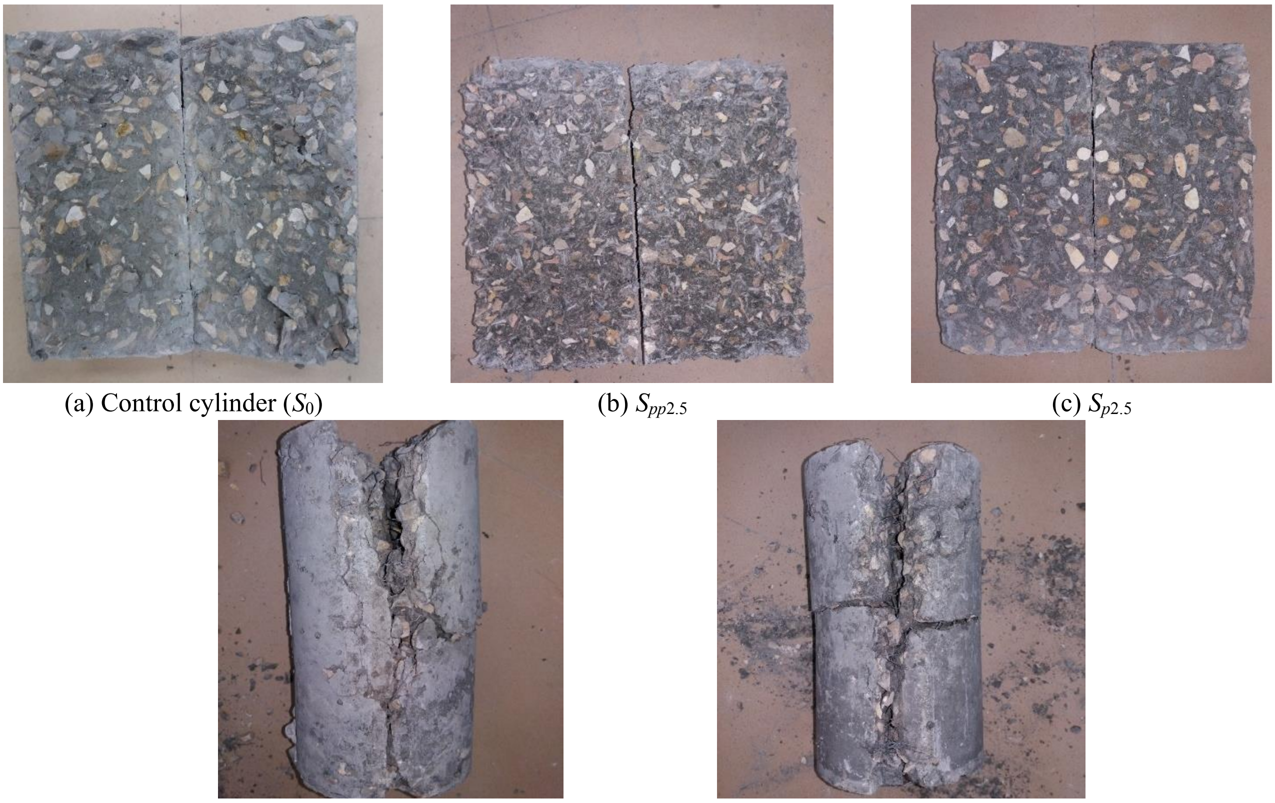

(a) Control cylinder (S_0) (b) $S_{pp2.5}$ (c) $S_{p2.5}$

(d) $S_{s2.5}$ (e) $S_{w2.5}$

Fig. 12 Failure modes of the tested cylinders under the splitting test

and $C_{w1.5}$, respectively, as illustrated in Fig. 10. The standard deviation of the mean between the compressive strength and toughness of concrete cubes reinforced with 1.5% volume fraction were 6.52 and 0.329.

In case of 2.5 % volume fraction, it was clear that cubes reinforced with the end-hooked steel fiber was better than the other three cubes in terms of the compressive strength, toughness, strains and elasticity modulus, as illustrated in Fig. 11. Moreover, the compressive strength and toughness of concrete cubes reinforced with 2.5% volume fraction exhibited the highest standard deviation of the mean of 8.57 and 0.405, respectively. From the above results, it was preferred to use the fibers in the following order: (1) the end-hooked steel, the rounded steel or the plastic fiber if the volume fraction equal to 0.5% (2) the end-hooked steel or the plastic fiber for volume fraction equal to 1.5% (3) the end-hooked steel fiber in case of the volume fraction equal to 2.5%.

4.2 Splitting tensile tests

Table 6 lists the results of the cylinders subjected to splitting tensile test. Eq. (3) specified by recommendations of ACI (318-11) was used to estimate the tensile strength of the concrete (f_t)

$$f_t = \frac{2F}{\pi dL} \tag{3}$$

where F is the ultimate splitting load, d is the cylinder diameter (150 mm), and L is the cylinder height (300 mm). Fig. 12 shows the failure modes of the tested cylinders. At the end of the splitting tensile test, the cylinder was fell under the influence of its weight from a height of 30 cm several times to be separated into two halves. The concrete surface of both the control specimen and the specimens including polypropylene fiber was level, as shown in Fig.

Table 6 Results of the cylinders subjected to splitting tensile

Beam notation	Splitting load, F (kN)	Tensile strength, f_t (N/mm^2)	Fiber effect		Failure mode
			Increase in f_t%	Decrease in f_t%	
S_0	188.3	2.66	--	--	Level surface, Self-separation at the splitting load
$S_{pp0.15}$	195.81	2.77	4.0	--	Very level surface, easy-separation after the splitting load
$S_{pp0.5}$	219.67	3.109	16.67	--	
$S_{pp1.5}$	202.65	2.868	7.63	--	
$S_{pp2.5}$	169.70	2.4	--	9.87	
$S_{p0.5}$	189.17	2.67	0.47	--	Curly surface, Easy separation after the splitting load due to plastic cut
$S_{p1.5}$	136.42	1.93	--	27.54	
$S_{p2.5}$	135.76	1.92	--	27.89	
$S_{s0.5}$	254.87	3.607	35.36	--	Curly surface, Very difficult separation after the splitting load because the end-hooked steel fiber well tied the two halves together
$S_{s1.5}$	264.77	3.75	40.62	--	
$S_{s2.5}$	280.45	3.97	48.95	--	
$S_{w0.5}$	183.60	2.6	--	2.48	Curly surface, no separation occurred because the round steel fiber well tied the two halves together and prevented the separation
$S_{w1.5}$	177.84	2.52	--	5.54	
$S_{w2.5}$	173.94	2.46	--	7.52	

(a) Control beam (B_{p0}) and three fibrous PC beams (b) $B_{p0.5}$, $B_{p1.5}$ and $B_{p2.5}$

Fig. 13 Failure modes of the PC beams under the flexure test

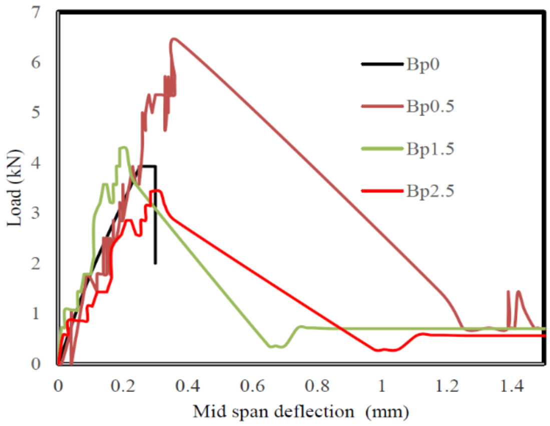

Fig. 14 Load-deflection relationships of the PC beams

Table 7 Results of the PC beams

Beam	P_u (kN)	Increase in P_u (%)	Δ_u (mm)	Increase in Δ_u (%)	Stiffness $k=P_u/\Delta_u$ (kN/mm)	Increase in k (%)	Toughness T (mm.kN)	Increase in T (%)
B_{p0}	3.93	--	0.25	--	15.6	--	0.68	--
$B_{p0.5}$	6.43	63.61	0.37	48	17.35	11.22	4.83	610.29
$B_{p1.5}$	4.28	8.90	0.21	-16	20.38	30.64	1.5	120.59
$B_{p2.5}$	3.43	-12.72	0.32	28	10.71	-31.35	1.71	151.47

12(a) and Fig. 12(b). The Curly surface was occurred in the plastic specimens after few falls of the cylinder, as shown in Fig. 12(c). The cylinders including end-hooked and rounded steel fibers were not separated after many precipitation times due to good contact, as shown in Fig. 12(d) and Fig. 12(e). It was noticed that using polypropylene fibers with volume fraction of 0.5% increased the tensile strength of the concrete by 16.67% compared to control specimen. It was preferred that polypropylene fibers not exceed 1.5% of the concrete volume. The use of plastic fibers with volume fraction higher than 0.5% decreased the tensile strength of the concrete On the other hand, the end-hooked steel fiber with volume fractions of 0.5, 1.5 and 2.5% increased the tensile strength of the concrete by 35.36, 40.62 and 48.95%, respectively. All concrete cylinders reinforced with rounded steel fibers yielded splitting tensile strength lower than the control cylinder (without fiber).

4.3 Beams tests

4.3.1 PC beams

Fig. 13 illustrates the failure modes of the PC beams subjected to flexure test. All PC beams vertically cracked at the mid span and separated to two halves, as shown in Fig. 13(a). All beams reinforced with recycled plastic fibers took more time than the control beam to fail because the recycled plastic fiber prevented the crack to open, as shown in Fig. 13(b). Results showed that the plastic delayed the failure of the PC beams due to crack bridging.

Load-mid span deflection relationships of the PC beams were shown in Fig. 14. The control beam (B_{P0}) directly failed at the maximum load while the fibrous beams resisted for more deflection after the maximum load, as shown in Fig. 14. Table 7 shows the results of the PC beams. Stiffness (k) was defined as the slope of the straight line from the original point to the maximum load while the toughness (T) was estimated as the area under the load-deflection curve up to 1.5 mm. The ultimate load (P_u) of the beams $B_{p0.5}$ and $B_{p1.5}$ was 63.61 and 8.9%, respectively, higher than the control beam B_{p0}. The P_u of the beam $B_{p2.5}$ was 12.72 lower than the B_{p0} beam. Accordingly, it was recommended that the volume fraction of the plastic fiber not exceed 1.5%. As the recycled plastic fibers volume fraction increased, the stiffness of the PC beams increased up to 1.5% then decreased. The beam $B_{p0.5}$, with recycled plastic fiber of 0.5%, had the highest ultimate load and toughness among all tested PC beams. Therefore, recycled plastic fibers with volume fraction of 0.5% was considered the optimum volume fraction for reinforcing the PC beams.

4.3.2 RC beams

Fig. 15 presents the failure modes of the RC beams subjected to flexure test. For both the control beam B_{R0} and the beam $B_{R2.5}$, the shear cracks occurred and increased with the loading. In these beams, the concrete cover separation (CCS) took placed at the maximum load, as shown in Fig. 15(a) and Fig. 15(d). The CCS appeared along a distance higher than the half span. The cracks of the $B_{R0.5}$ were shown in Fig. 15(b). The CCS took place before the shear crack so the $B_{R0.5}$ could not carry ultimate load higher than the control beam B_{R0}. For the $B_{R1.5}$ shown in Fig. 15(c), the failure was occurred due to CCS. Reason of the CCS occurrence was the absence of the transversal steel. Without stirrups, the recycled plastic fibers had a negative effect on the ultimate load capacity of the RC beams.

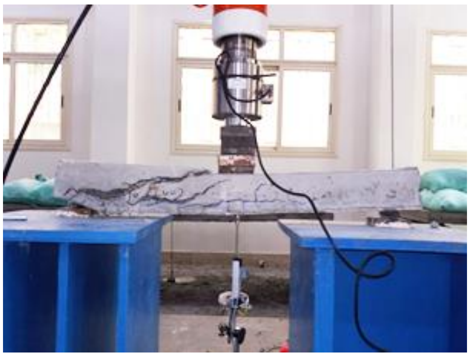

(a) Control beam (B_{R0})

(b) $B_{R0.5}$

(c) $B_{R1.5}$

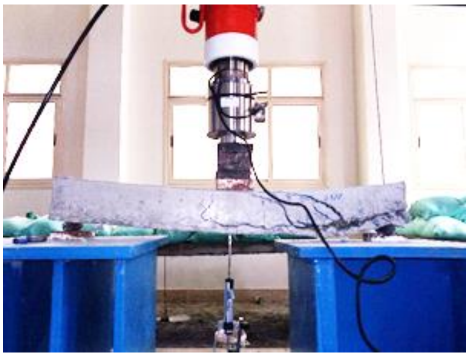

(d) $B_{R2.5}$

Fig. 15 Failure modes of the RC beams under the flexure test

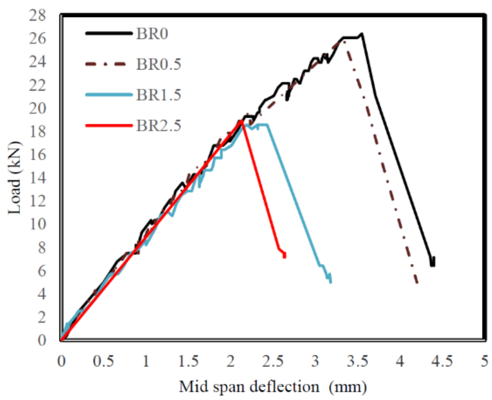

Fig. 16 Load-deflection relationships of the RC beams

Load-deflection relationships of the RC beams were shown in Fig. 16. The control beam B_{R0} and the fibrous beams resisted for more deflection after the maximum load. Table 8 lists the results of the RC beams. The P_u of the beams $B_{R0.5}$, $B_{R1.5}$ and $B_{R2.5}$ was 0.23, 28.78 and 27.39%, respectively, less than the B_{R0} beam. As the volume fraction of the recycled plastic fibers increased, the stiffness of the RC beams improved. The toughness of both the control beam B_{R0} and the $B_{R0.5}$ were approximately identical while the toughness of beams $B_{R1.5}$ and $B_{R2.5}$ were 50% less than the control beam B_{R0}. Therefore, the best volume fraction of the recycled plastic fibers was preferred to equal 0.5%.

4.4 The columns tests

4.4.1 PC columns

Fig. 17 shows the failure modes of all PC columns

(a) $P_{p1.5}$

(b) $P_{p2.5}$

Fig. 17 Failure modes of the PC columns

except the control column (P_{p0}) because of the P_{p0} was crushed to many parts at the maximum load and fall off. The control PC column suddenly ruptured with high sound. As illustrated in Fig. 17, the two fibrous columns did not crush at the maximum load due to the recycled plastic existing. A vertical crack took place and divided the column into two equal halves. As the load increased, cracks of fibrous RC columns widely opened but the recycled plastic fibers resisted the separation. Presence of the recycled plastic fibers with different volume fractions within the concrete matrix of the PC columns improved and delayed the failure. Fig. 18 presents the relationships between the

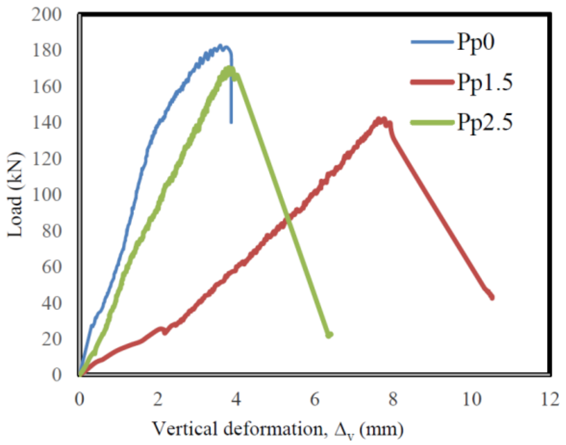

Fig. 18 Axial load-deformation relationships of the PC columns

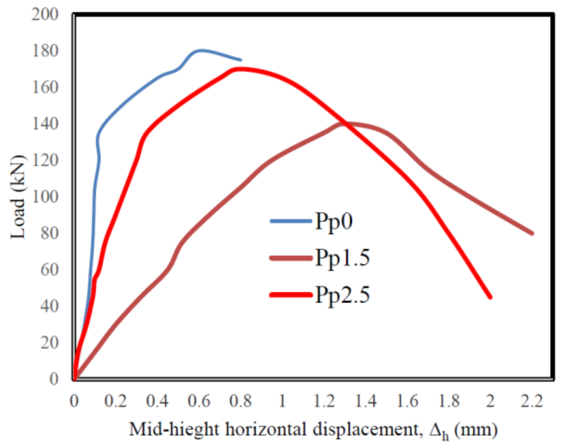

Fig. 19 Axial load-mid height side sway relationships of the PC columns

Table 8 Results of the RC beams

Beam	P_u (kN)	Decrease in P_u (%)	Δ_u (mm)	Decrease in Δ_u (%)	Stiffness $k=P_u/\Delta_u$ (kN/mm)	Increase in k (%)	Toughness T (mm.kN)	Decrease in T (%)
B_{R0}	26.06	--	3.33	--	7.82	--	57.33	--
$B_{R0.5}$	26.0	0.23	3.33	0.00	7.81	-0.89	54.60	4.76
$B_{R1.5}$	18.56	28.78	2.19	34.23	8.48	+8.44	29.51	48.52
$B_{R2.5}$	18.92	27.39	2.13	36.03	8.88	13.55	24.97	56.44

axial load and the vertical deformation (Δ_v) of the PC columns. Table 9 summarizes the results of the PC columns. It was noticed that the recycled plastic fibers decreased both the ultimate load and the stiffness of the PC columns while increased the toughness of the PC columns. Also, the recycled plastic fibers improved the ductility of the PC columns. Fig. 19 shows the axial load-mid height side sway relationships of the PC columns. It was showed that behavior of the PC column improved by using the recycled plastic fibers. The fibrous columns had ductility higher than that of the control column.

4.4.2 RC columns

Fig. 20 shows the failure modes of all RC columns. The control column (P_{R0}) had one longitudinal crack, as shown in Fig. 20(a), while many vertical cracks occurred in the fibrous column ($P_{R1.5}$), as shown in Fig. 20(b). The concrete cover of the P_{R0} fall off unlike the $P_{R1.5}$. The recycled plastic fibers in the RC columns improved and delayed the columns collapse. The Axial Load-deformation relationships of the RC columns were shown in Fig. 21. The deformation of the columns gradually increased until the ultimate deformation (Δ_{vu}) then suddenly dropped due to the crack open. The capacity of the columns continued with constant value until the test end because of the confinement

(a) P_{R0} (b) $P_{R1.5}$

Fig. 20 Failure modes of the RC columns

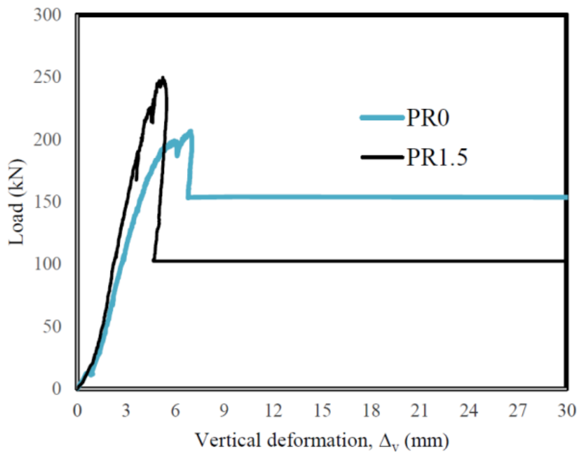

Fig. 21 Axial load-deformation relationships of the RC columns

Table 9 Results of the PC columns

Column	P_u (kN)	Decrease in P_u (%)	Δ_{vu} (mm)	Increase in Δ_{vu} (%)	Stiffness $k=Pu/\Delta u$ (kN/mm)	Decrease in k (%)	Toughness T (mm.kN)	Increase in T (%)
P_{p0}	181.35	--	3.78	--	47.97	--	342.75	--
$P_{p1.5}$	138.16	23.81	7.82	106.87	17.66	63.18	727.41	112.22
$P_{p2.5}$	167.43	7.67	3.78	0.00	44.29	7.67	532.43	55.34

Table 10 Results of the RC columns

Column	P_u (kN)	Increase in P_u (%)	Δ_{vu} (mm)	Decrease in Δ_{vu} (%)	Stiffness k=line slope (kN/mm)	Increase in k (%)	Toughness T up to Δ_v =30 mm (mm.kN)	Decrease in T (%)
P_{R0}	201.70	--	7.02	--	53.16	--	4186.46	--
$P_{R1.5}$	244.9	21.42	5.40	23.08	61.41	15.52	3730	10.9

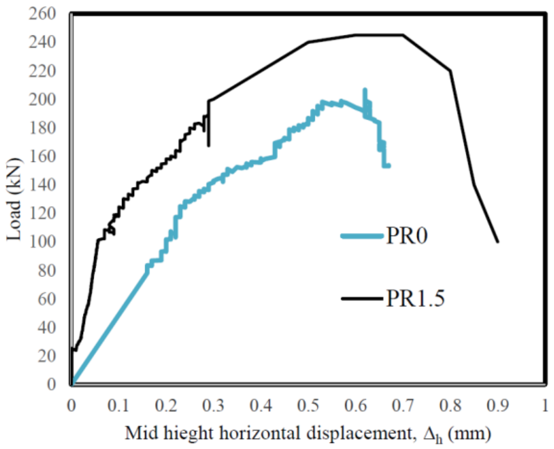

Fig. 22 Axial ;oad-mid height side sway relationships of the RC columns

of reinforcement and concrete occurred because of stirrups which prevented the cracks to open. The results analysis of RC columns was proposed and listed in Table 10. The ultimate load and the stiffness of the $P_{R1.5}$ were 21.42 and 15.52%, respectively, higher than the control column P_{R0}. On the other hand, the toughness of the $P_{R1.5}$ was 10.9% lower than the P_{R0}. The axial load versus the side sway at the mid height of the RC columns was drawn in Fig. 22. The recycled plastic fiber had a significant effect on both the ductility and toughness of the RC columns. The toughness of the $P_{R1.5}$ was higher than the control RC column P_{R0}.

5. Conclusions

The current research investigated the hardened state mechanical properties of concrete matrix reinforced with different types of fibers i.e., steel, polypropylene and recycled plastic of 0.5%, 1.5% and 2.5% volume fractions. Based on the experimental findings, the conclusions can be drawn as follows:

1. The Results of the splitting tensile tests indicated that specimens reinforced with polypropylenes and recycled plastic fibers easily separated in contrast to steel fibers which prevented the separation. Moreover, as the volume fraction of both polypropylene and recycled plastic fibers increased, the splitting tensile strength of fibrous concrete increased up to 1.5% and 0.5%, respectively and then decreased. As the end-hooked steel fiber volume fractions increased the splitting tensile strength of concrete increased. On the contrary, the rounded steel fibers had a negative effect on the splitting tensile strength.
2. As the polypropylene fibers volume fraction increased, the compressive strength of concrete increased up to 0.15% then decreased. Presence of the end-hooked steel fibers with volume fraction over 0.5% significantly enhanced the compressive strength of concrete matrix compared to the control cube. Both the recycled plastic fibers and the rounded steel fibers had a negative effect on the compressive strength of concrete. The inclusion of fibers into concrete significantly improved the compressive toughness.
3. Reinforcing the plain concrete beams with recycled plastic fiber controlled the crack opening and increased both the flexural capacity and toughness in comparison with the un-reinforced beam. At 0.5%, the flexural capacity and toughness improved with 63% and 610%, respectively compared to the reference PC beam. On the other hand, the recycled plastic fibers had a negative impact on the shear performance of RC beams without shear reinforcement.
4. The recycled plastic fibers prevented the highly sounded sudden and brittle rupture of PC columns and increased both toughness and maximum shortening displacement however it decreased the maximum ultimate load and stiffness. Reinforcing RC column with recycled plastic fibers of 1.5% volume fraction increased numbers of the vertical cracks along the column face and prevented the concrete cover splitting compared to one longitudinal crack in case of the control RC column. Moreover, the maximum ultimate load and stiffness of $P_{R1.5}$ increased by 21% and 15%, respectively compared to P_{R0}.

Acknowledgements

The experimental program was tested at the reinforced concrete laboratory of the faculty of Engineering, Kafrelsheikh University, Egypt.

Declaration of conflicting interests

The authors declared no potential conflicts of interest with respect to the research, authorship, and/or publication of this article.

References

ACI Committee (2011), Building Code Requirements for Structural Concrete (ACI 318-11), American Concrete Institute.

Abbass, W., Khan, M.I. and Mourad, S. (2018), "Evaluation of mechanical properties of steel fiber reinforced concrete with different strengths of concrete", *Constr. Build. Mater.*, **168**, 556-569. https://doi.org/10.1016/j.conbuildmat.2018.02.164.

Akcay, B. and Ozsar, D.S. (2019), "Do polymer fibres affect the distribution of steel fibres in hybrid fibre reinforced concretes?", *Constr. Build. Mater.*, **228**, 116732. https://doi.org/10.1016/j.conbuildmat.2019.116732.

Al-Masoodi, A.H.H., Kawan, A., Kasmuri, M., Hamid, R. and Khan, M.N.N. (2016), "Static and dynamic properties of concrete with different types and shapes of fibrous reinforcement", *Constr. Build. Mater.*, **104**, 247-262. https://doi.org/10.1016/j.conbuildmat.2015.12.037.

Alwesabi, E.A.H., Bakar, B.H.A., Alshaikh, I.M.H. and Akil, H.M. (2020), "Experimental investigation on mechanical properties of plain and rubberised concretes with steel–polypropylene hybrid fibre", *Constr. Build. Mater.*, **233**, 117194. https://doi.org/10.1016/j.conbuildmat.2019.117194.

Ashok, M., Jayabalan, P., Saraswathy, V. and Muralidharan, S. (2020), "A study on mechanical properties of concrete including activated recycled plastic waste", *Adv. Concrete Constr.*. **9**(2), 207-2015. https://doi.org/10.12989/acc.2020.9.2.207.

Bayramov, F., Taşdemir, C. and Taşdemir, M.A. (2004), "Optimisation of steel fibre reinforced concretes by means of statistical response surface method", *Cement Concrete Compos*., **26**(6), 665-675. https://doi.org/10.1016/S0958-9465(03)00161-6.

Charron, J.P., Desmettre, C. and Androuët, C. (2020), "Flexural and shear behaviors of steel and synthetic fiber reinforced concretes under quasi-static and pseudo-dynamic loadings", *Constr. Build. Mater*., **238**, 117659. https://doi.org/10.1016/j.conbuildmat.2019.117659.

Elices, M. and Rocco, C.G. (2008), "Effect of aggregate size on the fracture and mechanical properties of a simple concrete", *Eng. Fract. Mech*., **75**(13), 3839-3851. https://doi.org/10.1016/j.engfracmech.2008.02.011.

Fu, C., Ye, H., Wang, K., Zhu, K. and He, C. (2019), "Evolution of mechanical properties of steel fiber-reinforced rubberized concrete (FR-RC)", *Compos. Part B: Eng*., **160**, 158-166. https://doi.org/10.1016/j.compositesb.2018.10.045.

Gomes, R.F., Dias, D.P. and de Andrade Silva, F. (2020), "Determination of the fracture parameters of steel fiber-reinforced geopolymer concrete", *Theo. Appl. Fract. Mech*., **107**, 102568. https://doi.org/10.1016/j.tafmec.2020.102568.

Grünewald, S. and Walraven, J.C. (2001), "Parameter-study on the influence of steel fibers and coarse aggregate content on the fresh properties of self-compacting concrete", *Cement Concrete Res*., **31**(12), 1793-1798. https://doi.org/10.1016/S0008-8846(01)00555-5.

Grzymski, F., Musiał, M. and Trapko, T. (2019), "Mechanical properties of fibre reinforced concrete with recycled fibres", *Constr. Build. Mater*., **198**, 323-331. https://doi.org/10.1016/j.conbuildmat.2018.11.183.

Guo, H., Tao, J., Chen, Y., Li, D., Jia, B. and Zhai, Y. (2019), "Effect of steel and polypropylene fibers on the quasi-static and dynamic splitting tensile properties of high-strength concrete", *Constr. Build. Mater*., **224**, 504-514. https://doi.org/10.1016/j.conbuildmat.2019.07.096.

Han, J., Zhao, M., Chen, J. and Lan, X. (2019), "Effects of steel fiber length and coarse aggregate maximum size on mechanical properties of steel fiber reinforced concrete", *Constr. Build. Mater*., **209**, 577-591. https://doi.org/10.1016/j.conbuildmat.2019.03.086.

Khan, M., Cao, M. and Ali, M. (2020), "Cracking behaviour and constitutive modelling of hybrid fibre reinforced concrete", *J. Build. Eng*., **30**, 101272. https://doi.org/10.1016/j.jobe.2020.101272.

Lee, S.J., Hong, Y., Eom, A.H. and Won, J.P. (2018), "Effect of steel fibres on fracture parameters of cementitious composites", *Compos. Struct*., **204**, 658-663. https://doi.org/10.1016/j.compstruct.2018.08.002.

Liu, F., Ding, W. and Qiao, Y. (2020), "Experimental investigation on the tensile behavior of hybrid steel-PVA fiber reinforced concrete containing fly ash and slag powder", *Constr. Build. Mater*., **241**, 118000. https://doi.org/10.1016/j.conbuildmat.2020.118000.

Mazloom, M., Karimpanah, H. and Karamloo, M. (2020), "Fracture behavior of monotype and hybrid fiber reinforced self-compacting concrete at different temperatures", *Adv. Concrete Constr*., **9**(4), 375-386. https://doi.org/10.12989/acc.2020.9.4.375.

Mohammadhosseini, H., Tahir, M.M., Alaskar, A., Alabduljabbar, H. and Alyousef, R. (2020), "Enhancement of strength and transport properties of a novel preplaced aggregate fiber reinforced concrete by adding waste polypropylene carpet fibers", *J. Build. Eng*., **27**, 101003. https://doi.org/10.1016/j.jobe.2019.101003.

Mohammed, A.A. and Rahim, A.A.F. (2020), "Experimental behavior and analysis of high strength concrete beams reinforced with PET waste fiber", *Constr. Build. Mater*., **244**, 118350. https://doi.org/10.1016/j.conbuildmat.2020.118350.

Murthy, A.R. and Ganesh, P. (2019), "Effect of steel fibres and nano silica on fracture properties of medium strength concrete", *Adv. Concrete Constr.*, **7**(3), 143-150. DOI: https://doi.org/10.12989/acc.2019.7.3.143.

Pal, S., Shariq, M., Abbas, H., Pandit, A.K. and Masood, A. (2020), "Strength characteristics and microstructure of hooked-end steel fiber reinforced concrete containing fly ash, bottom ash and their combination", *Constr. Build. Mater*., **247**, 118530.

Pešić, N., Živanović, S., Garcia, R. and Papastergiou, P. (2016), "Mechanical properties of concrete reinforced with recycled HDPE plastic fibres", *Constr. Build. Mater*., **115**, 362-370. https://doi.org/10.1016/j.conbuildmat.2020.118530.

Sabapathy, Y.K., Sabarish, S., Nithish, C.N.A., Ramasamy, S.M. and Krishna, G. (2019), "Experimental study on strength properties of aluminium fibre reinforced concrete", *J. King Saud Univ.-Eng. Sci.*. https://doi.org/10.1016/j.jksues.2019.12.004.

Sengul, O. (2016), "Mechanical behavior of concretes containing waste steel fibers recovered from scrap tires", *Constr. Build. Mater*., **122**, 649-658. https://doi.org/10.1016/j.conbuildmat.2016.06.113.

Shen, D., Liu, X., Zeng, X., Zhao, X. and Jiang, G. (2020), "Effect of polypropylene plastic fibers length on cracking resistance of high performance concrete at early age", *Constr. Build. Mater*., **244**, 117874. https://doi.org/10.1016/j.conbuildmat.2019.117874.

Shi, X., Park, P., Rew, Y., Huang, K. and Sim, C. (2020), "Constitutive behaviors of steel fiber reinforced concrete under uniaxial compression and tension", *Constr. Build. Mater*., **233**, 117316. https://doi.org/10.1016/j.conbuildmat.2019.117316.

Sivakumar, A. and Santhanam, M. (2007), "Mechanical properties of high strength concrete reinforced with metallic and non-metallic fibres", *Cement Concrete Compos*., **29**(8), 603-608. https://doi.org/10.1016/j.cemconcomp.2007.03.006.

Song, P.S. and Hwang, S. (2004), "Mechanical properties of high-strength steel fiber-reinforced concrete", *Constr. Build. Mater*., **18**(9), 669-673. https://doi.org/10.1016/j.conbuildmat.2004.04.027.

Thomas, J. and Ramaswamy, A. (2007), "Mechanical properties of steel fiber-reinforced concrete", *J. Mater. Civil Eng.*. **19**(5), 385-392. https://doi.org/10.1061/(ASCE)0899-1561(2007)19:5(385).

Trottier, J.F. and Banthia, N. (1994), "Toughness characterization of steel-fiber reinforced concrete", *J. Mater. Civil Eng*., **6**(2), 264-289. https://doi.org/10.1061/(ASCE)0899-1561(1994)6:2(264).

Zhang, P., Li, Q. and Sun, Z. (2012), "Effect of polypropylene fibre on flexural properties of concrete composites containing fly ash and silica fume", *Proc. Inst. Mech. Eng., Part L: J. Mater.: Des. Appl*, **226**(2), 177-181. https://doi.org/10.1177/1464420712437637.

Zhong, H. and Zhang, M. (2020), "Experimental study on engineering properties of concrete reinforced with hybrid recycled tyre steel and polypropylene fibres", *J. Clean. Prod*., **259**, 120914. https://doi.org/10.1016/j.jclepro.2020.120914.

CC